RSC Advances

This article can be cited before page numbers have been issued, to do this please use: K. Ghosh, R. Kumar, S. Kumar, M. Bala, A. Ratnam and U. P. Singh, *RSC Adv.*, 2016, DOI: 10.1039/C6RA17223G.

ROYAL SOCIETY OF CHEMISTRY

www.rsc.org/advances

View Article Online
DOI: 10.1039/C6RA17223G

Journal Name

ARTICLE

Site-specific orthometallation *via* C–H bond activation and syntheses of ruthenium (III) organometallics: Studies on nitric oxide (NO) reactivity and photorelease of coordinated NO

Received 00th January 20xx,
Accepted 00th January 20xx

DOI: 10.1039/x0xx00000x

www.rsc.org/

Rajan Kumar, Sushil Kumar, Manju Bala, Anand Ratnam, U. P. Singh, and Kaushik Ghosh*

A new family of σ-aryl ruthenium(III) complexes [Ru(L^{1-4})(PPh_3)$_2$Cl] (**1–4**) (where L^1H_2 = *N*-(quinolin-8-yl)benzamide for **1**, L^2H_2 = 4-chloro-*N*-(quinolin-8-yl)benzamide for **2**, L^3H_2 = 4-nitro-*N*-(quinolin-8-yl)benzamide for **3**, L^4H_2 = 3-nitro-*N*-(quinolin-8-yl)benzamide for **4** and H = dissociable protons) derived from the bidentate ligands having amide bond were synthesized through C–H bond activation. These organometallic ruthenium(III) complexes were treated with nitric oxide (NO) to afford the nitrosyl complexes [Ru(NO_2L^{1-4})(PPh_3)$_2$(NO)](ClO_4) (**1a–4a**) (where $NO_2L^1H_2$ = *N*-(5-nitroquinolin-8-yl)benzamide for **1a**, $NO_2L^2H_2$ = 4-chloro-*N*-(5-nitroquinolin-8-yl)benzamide for **2a**, $NO_2L^3H_2$ = 4-nitro-*N*-(5-nitroquinolin-8-yl)benzamide for **3a**, $NO_2L^4H_2$ = 3-nitro-*N*-(5-nitroquinolin-8-yl)benzamide for **4a** and H = dissociable protons). All ruthenium complexes were characterized by various spectroscopic studies. X-ray crystallographic study afforded the molecular structure of the complex **4a** and the site-specific orthometallation was scrutinized. Coordinated NO molecule was found to be photolabile under visible as well as UV light.

Introduction

A plentiful literatures are available for ruthenium (II) and ruthenium (III) organometallic complexes because of their immense importance for organometallic and organic syntheses.[1–5] There has been considerable current interest in the design and synthesis of nitric oxide releasing molecules (NORM) for target specific and on demand delivery of nitric oxide(NO).[6–17] A marked feature of ruthenium chemistry is the formation of nitric oxide complex[18] however, organometallic complexes used for nitric oxide (NO) donation are scarce in the literature.[19–22] Investigation of chemistry of ruthenium nitrosyls clearly indicated the stability of complexes having {RuNO}^{6} (according to Enemark Feltham notation)[6] moiety. Among several routes, synthetically this could be achieved by a combination of Ru(III) centre and NO. Hence, recently we have communicated Ru(III) organometallics and studied their reactivity with NO. Our previous reports clearly indicated that a bidentate ligand having N_{imine} and O_{phenol} donors (LH_2 and $L'H_2$) (shown in Scheme 1 and 2) afforded C–H bond activation and orthometallation.[20–23] There are two important aspects of our previous results in terms of the synthesis of NORM derived from organometallic ruthenium complexes which were taken into account for the design and synthesis of new ligands achieving the synthesis of Ru(III) organometallics and corresponding ruthenium nitrosyls. First, synthesis of Ru(III) organometallics *via* C–H bond activation using a Ru(II) precursor complex and consequently conversion of bidentate ligands to tridentate ligands, hence donor atoms present in bidentate ligands are extremely important. Second, reactivity of nitric oxide with ruthenium(III) organometallics and the role of the *trans* directing effect of carbanion for the coordination and photolability of NO. These results prompted us to design and synthesize new bidentate ligands which would enhance the oxidation of ruthenium centre (II to III) and concomitant Ru–C bond formation *via* C–H bond activation and the synthesis of new Ru(III) organometallics.

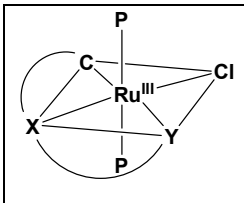

X	Y	Refs.
N_{azo}	O_{phenol}	24–27
N_{imine}	O_{phenol}	21–23, 28, 29
N_{imine}	O_{amide}	30–33
N_{amide}	$N_{pyridine}$	This work

Scheme 1. Donors (X and Y) in bidentate ligands.

Hence we designed bidentate ligands with $N_{pyridine}$ and N_{amide} donors ($L^{1-4}H_2$) (shown in Scheme 2) and ligands were reacted with Ru(II) precursor complex. Deprotonated carboxamido nitrogen is known to stabilize the higher oxidation state of metal centre.[34] Moreover, amide nitrogen

R. Kumar, S. Kumar, M. Bala, Prof. U.P. Singh, Dr. K. Ghosh
Department of Chemistry, Indian Institute of Technology, Roorkee, Roorkee-247667, Uttarakhand, INDIA
Fax: +91-1332-275547, E-mail: ghoshfcy@iitr.ernet.in
† Footnotes relating to the title and/or authors should appear here.
Electronic Supplementary Information (ESI) available: [details of any supplementary information available should be included here]. See DOI: 10.1039/x0xx00000x

View Article Online
DOI: 10.1039/C6RA17223G

exhibits trans effect and is known for coordination and photolability of nitric oxide.[7,35]

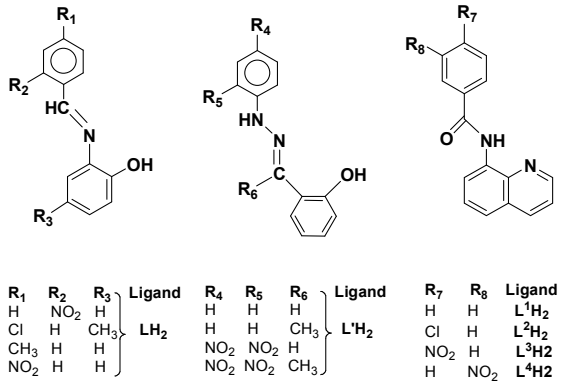

Scheme 2. Schematic drawing of ligands LH_2, $L'H_2$ and $L^{1-4}H_2$.

Herein, we designed bidentate ligands having amide bond and synthesized ligands L^nH_2 (where n= 1–4). A new family of σ-aryl ruthenium(III) complexes $[Ru(L^1)(PPh_3)_2Cl]$ (**1**), $[Ru(L^2)(PPh_3)_2Cl]$ (**2**), $[Ru(L^3)(PPh_3)_2Cl]$ (**3**) and $[Ru(L^4)(PPh_3)_2Cl]$ (**4**) (Scheme 3) (where L^1H_2 = *N*-(quinolin-8-yl)benzamide, L^2H_2 = 4-chloro-*N*-(quinolin-8- yl)benzamide, L^3H_2 = 4-nitro-*N*-(quinolin-8-yl)benzamide, L^4H_2 = 3-nitro-*N*-(quinolin-8-yl)benzamide and H = dissociable protons) were synthesized from these bidentate ligands containing carboxamido group (Scheme 2). Cyclometalated complexes were characterized by various spectroscopic techniques and the site-specific cyclometalation during C–H bond activation will be described in this report.

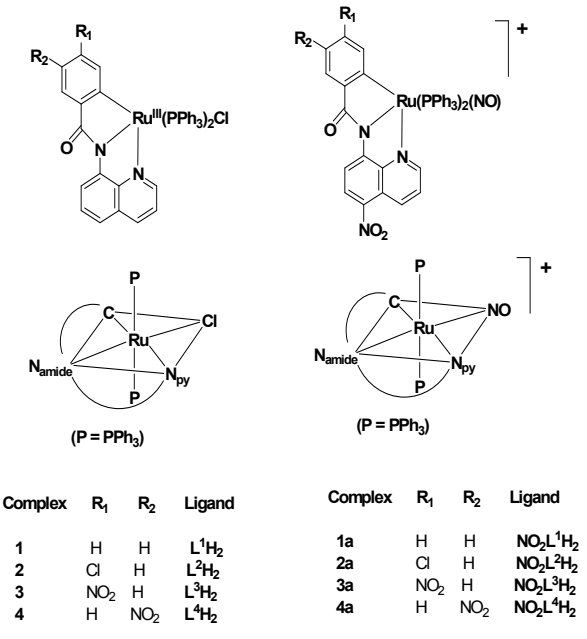

Complex	R_1	R_2	Ligand
1	H	H	L^1H_2
2	Cl	H	L^2H_2
3	NO_2	H	L^3H_2
4	H	NO_2	L^4H_2

Complex	R_1	R_2	Ligand
1a	H	H	$NO_2L^1H_2$
2a	Cl	H	$NO_2L^2H_2$
3a	NO_2	H	$NO_2L^3H_2$
4a	H	NO_2	$NO_2L^4H_2$

Scheme 3. Schematic drawings of cyclometalated ruthenium complexes.

The reactivity study of NO with ruthenium(III) complexes (**1–4**) was performed to afford cyclometalated ruthenium nitrosyl complexes $[Ru(NO_2L^1)(PPh_3)_2(NO)](ClO_4)$ (**1a**, where $NO_2L^1H_2$ = *N*-(5-nitroquinolin-8-yl)benzamide and H = dissociable protons), $[Ru(NO_2L^2)(PPh_3)_2(NO)](ClO_4)$ (**2a**, where $NO_2L^2H_2$ = 4-chloro-*N*-(5-nitroquinolin-8-yl) benzamide and H = dissociable protons), $[Ru(NO_2L^3)(PPh_3)_2(NO)]$ (ClO_4) (**3a**, where $NO_2L^3H_2$ = 4-nitro-*N*-(5-nitroquinolin-8-yl)benzamide and H = dissociable protons) and $[Ru(NO_2L^4)(PPh_3)_2(NO)](ClO_4)$ (**4a**, where $NO_2L^4H_2$ = 3-nitro-*N*-(5-nitroquinolin-8-yl)benzamide and H = dissociable protons) (Scheme 3). The molecular structure of **4a** was determined by X-ray crystallography. The redox properties of the metal centre in all the complexes were investigated. The photolability of coordinated NO was performed by UV-Vis spectral studies and liberated NO was trapped by reduced myoglobin. Photoreleased NO was estimated by a Griess reagent using visible as well as UV light. The role of $–NO_2$ group (electron-withdrawing group) on the phenyl ring, chelated to the metal centre *via* σ-aryl bond, will be discussed in this paper of light-induced delivery of NO.

Experimental Section

Materials. All the chemicals used were of reagent grade. $RuCl_3.3H_2O$ was puchased from Loba Chemie Pvt. Ltd., Mumbai, India. Analytical grade reagents sodium nitrite, benzoic acid, 4-chlorobenzoic acid, 4-nitrobenzoic acid, 3-nitrobenzoic acid, naphthylethylenedi- amine dihydrochloride (NED), sulfanilamide, sodium perchlorate monohydrate, sodium nitrite (Himedia Laboratories Pvt. Ltd., Mumbai, India), quinoline-8-amine (Sigma Aldrich, Steinheim, Germany) were used as obtained. Triphenylphosphine (SRL,Mumbai, India), disodium hydrogen phosphate anhydrous (RFCL Ltd. New Delhi, India) and sodium dihydrogen phosphate (Chemport India Pvt. Ltd. Mumbai, India) were used as obtained. Double distilled water and distilled solvents were used in during the experiments. Equine skeletal muscle myoglobin was obtained from Sigma Aldrich, Steinheim, Germany.

Physical measurements. Infrared spectra were obtained as KBr pellets with Thermo Nicolet Nexus FT–IR spectrometer, using 16 scans and were reported in cm^{-1}. Electronic absorption spectra of all the complexes were recorded in dichloromethane solvent with an Evolution 600, Thermo Scientific (Shimadzu) UV–vis spectrophotometer. ^1H and ^{31}P NMR spectra were recorded on Bruker AVANCE, 500.13 MHz spectrometer in the deuterated solvents. Cyclic voltammetric studies were performed on a CH–600C electroanalyzer in dichloromethane with 0.1 M tetrabutylammonium perchlorate (TBAP) as supporting electrolyte. The working electrode, reference electrode and auxiliary electrode were glassy carbon electrode, Ag/AgCl electrode and Pt wire respectively. The concentration of the compounds was in the order of 10^{-3} M. The ferrocene/ferrocenium couple occurred at $E_{1/2}$ = + 0.54 (70) V *vs*. Ag/AgCl (scan rate 0.1 V/s) in dichloromethane under the same experimental conditions.

View Article Online
DOI: 10.1039/C6RA17223G

Syntheses of ligands:

Synthesis of *N*-(quinolin-8-yl)benzamide (L^1H_2): The benzoic acid (0.61 g, 5.0 mmol) was taken in 15-20 mL dimethylformaide solution and then cooled on an ice bath. To this solution, 1.48 g (11.0 mmol) of 1-hydroxybenzotriazole (HOBT) as well as 1.13 g (5.5 mmol) of dicyclohexylcarbodiimide (DCC) were added directly and mixture was stirred for half an hour at 0°C. Now a batch of quinoline-8-amine 0.72 g (5.0 mmol) was added to the reaction mixture with stirring for next 2 hours on the same ice bath. After, the ice bath was removed and the stirring was continued overnight at room temperature. By removing the white precipitate of N,N′-dicyclohexylurea through filtration, the solvent was concentrated to 10 mL. Within 3-4 days, a light yellowish crystalline solid of ligand L^1H_2 was settled down on the bottom of beaker which was filtered and washed with methanol and diethyl ether. Yield: 52%. Anal. Calcd. For $C_{16}H_{12}N_2O$ (248.29): C, 77.40; H, 4.87; N, 11.28. Found: C, 77.48; H, 4.38; N, 11.41. IR (KBr disk, cm^{-1}): 1674 (ν_{CO}, –CONH), 3350 ($\nu_{N–H}$). UV–Vis (CH_2Cl_2; λ_{max}, nm (ε, M^{-1} cm^{-1})): 242 (24166), 270 (6975), 325 (7333). ^1H NMR ($CDCl_3$, 500 MHz): δ 10.76 (s, 1H), 8.95 (t, 1H), 8.86 (s, 1H), 8.19 (d, 1H), 8.09 (t, 2H), 7.61-7.56 (m, 5H), 7.5 (t, 1H) ppm.

Synthesis of 4-chloro-*N*-(quinolin-8-yl)benzamide (L^2H_2): Ligand L^2H_2 was synthesized from the reaction of p-chloro benzoic acid with quinoline-8-amine by following the same procedure as for ligand L^1H_2. Yield: 61%. Anal. Calcd. For $C_{16}H_{11}ClN_2O$ (282.72): C, 67.97; H, 3.92; N, 9.91. Found: C, 66.90; H, 3.64; N, 9.98. IR (KBr disk, cm^{-1}): 1665 (ν_{CO}, –CONH), 3350 ($\nu_{N–H}$). UV–Vis (CH_2Cl_2; λ_{max}, nm (ε, M^{-1} cm^{-1})): 242 (23030), 275 (4970), 324 (6060). ^1H NMR ($CDCl_3$, 500 MHz): δ 10.68 (s, 1H), 8.89-8.82 (m, 2H), 8.15 (q, 1H), 8.01-7.98 (m, 2H), 7.58-7.44 (m, 5H) ppm.

Synthesis of 4-nitro-*N*-(quinolin-8-yl)benzamide (L^3H_2): Ligand L^3H_2 was prepared from the reaction of p-nitro benzoic acid with quinoline-8-amine by using the same procedure as for ligand L^1H_2. Yield: 68%. Anal. Calcd. For $C_{16}H_{11}N_3O_3$ (293.28): C, 65.53; H, 3.78; N, 14.33. Found: C, 65.38; H, 3.46; N, 14.43. IR (KBr disk, cm^{-1}): 1675 (ν_{CO}, –CONH), 3350 ($\nu_{N–H}$). UV–Vis (CH_2Cl_2; λ_{max}, nm (ε, M^{-1} cm^{-1})): 242 (25017), 335 (6084). ^1H NMR ($CDCl_3$, 500 MHz): δ 10.81 (s, 1H), 8.91-8.86 (m, 2H), 8.39-8.36 (m, 2H), 8.24-8.21 (m, 3H), 7.63-7.50 (m, 3H) ppm.

Synthesis of 3-nitro-*N*-(quinolin-8-yl)benzamide (L^4H_2): Ligand L^4H_2 was obtained from the reaction of m-nitro benzoic acid and quinoline-8-amine through the same procedure as for ligand L^1H_2. Yield: 71%. Anal. Calcd. For $C_{16}H_{11}N_3O_3$ (293.28): C, 65.53; H, 3.78; N, 14.33. Found: C, 65.38; H, 3.43; N, 14.52. IR (KBr disk, cm^{-1}): 1670 (ν_{CO}, –CONH), 3307 ($\nu_{N–H}$). UV–Vis (CH_2Cl_2; λ_{max}, nm (ε, M^{-1} cm^{-1})): 242 (23734), 262 (9769), 325 (8146). ^1H NMR ($CDCl_3$, 500 MHz): δ 10.79 (s, 1H), 8.89-8.85 (m, 3H), 8.42-8.37 (m, 2H), 8.19 (q, 1H), 7.73 (t, 1H), 7.61-7.48 (m, 3H) ppm.

Syntheses of cyclometalated ruthenium complexes

The precursor complex $[Ru(PPh_3)_3Cl_2]$ was prepared by using the reported procedure.[20–22,36]

Caution: perchlorate salts of metal complexes with organic ligands are potentially explosive. Only a small amount of material should be prepared and handled with caution.

Synthesis of $[Ru(L^1)(PPh_3)_2(Cl)]$ (1): To a 30 mL methanolic solution of L^1H_2 (0.034 g, 0.12 mmol) was added directly ruthenium precursor complex $[Ru(PPh_3)_3Cl_2]$ (0.0958g, 0.10 mmol) and mixture was refluxed at 85°C for 10–12 h on an oil bath to afforded a light brown crystalline solid at room temperature and was washed with cold methanol and diethyl ether. Yield: 48%. Anal. Calcd. for $C_{52}H_{40}ClN_2OP_2Ru$ (907.13): C, 68.83; H, 4.44; N, 3.09. Found: C, 68.48; H, 4.38; N, 3.12. IR (KBr disk, cm^{-1}): 1558 (ν_{CONH}), 746, 692, 520 (ν_{PPh3}) cm^{-1}. UV-Vis (CH_2Cl_2; λ_{max}/nm (ε, $M^{-1}cm^{-1}$)): 270 (17280), 335 (4041), 445 (1942).

Synthesis of $[Ru(L^2)(PPh_3)_2(Cl)]$ (2): Complex **2** was synthesized through the reaction of $[Ru(PPh_3)_3Cl_2]$ with the ligand L^2H_2 by following the same procedure as for **1**. Yield: 58%. Anal. Calcd. for $C_{52}H_{39}Cl_2N_2OP_2Ru$ (941.10): C, 66.32; H, 4.17; N, 2.97. Found: C, 66.24; H, 4.09; N, 2.88. IR (KBr disk, cm^{-1}): 1635 (ν_{CONH}), 746, 694, 522 (ν_{PPh3}) cm^{-1}. UV-Vis (CH_2Cl_2; λ_{max}/nm (ε, $M^{-1}cm^{-1}$)): 262 (17596), 365 (2804).

Synthesis of $[Ru(L^3)(PPh_3)_2(Cl)]$ (3): Complex **3** was prepared with the help of ligand L^3H_2 through the same procedure as for **1**. Yield: 68%. Anal. Calcd. for $C_{52}H_{39}ClN_3O_3P_2Ru$ (952.12): C, 65.58; H, 4.13; N, 4.41. Found: C, 65.43; H, 4.08; N, 4.50. IR (KBr disk, cm^{-1}): 1632 (ν_{CONH}), 744, 694, 515 (ν_{PPh3}) cm^{-1}. UV-Vis (CH_2Cl_2; λ_{max}/nm (ε, $M^{-1}cm^{-1}$)): 274 (28626), 460 (5042).

Synthesis of $[Ru(L^4)(PPh_3)_2(Cl)]$ (4): Complex **4** was obtained by using ligand L^4H_2 by using the same procedure as for **1**. Yield: 62%. Anal. Calcd. For $C_{52}H_{39}ClN_3O_3P_2Ru$ (952.12): C, 65.58; H, 4.13; N, 4.41. Found: C, 65.38; H, 4.10; N, 4.52. IR (KBr disk, cm^{-1}): 1625 (ν_{CONH}), 742, 692, 514 (ν_{PPh3}) cm^{-1}. UV-Vis (CH_2Cl_2; λ_{max}/nm (ε, $M^{-1}cm^{-1}$)): 274 (25615), 365 (10570), 460 (4966).

Synthesis of $[Ru(NO_2L^1)(PPh_3)_2(NO)](ClO_4)$ (1a): A batch of (0.090 g, 0.1 mmol) of complex **1** was taken in 30 mL of dichloromethane to obtain a yellow colored solution in round bottom flask of 100 mL. Now 25 mL acidified distilled water was layered over this solution. Sodium nitrite (0.3 g, 4.3 mmol) was added to the bilayer solution and the mixture was stirred at room temperature for 2 hrs to get reddish yellow colored solution of complex **1a**. The dichloromethane layer was separated out and $NaClO_4$ (in excess) with 10 mL of methanol was added to this solution. Stirring of this solution was continued for another 2 hour. The solvent mixture was evaporated to get reddish yellow solid. To remove excess of $NaClO_4$, this solid was further dissolved in 10 mL of dichloromethane and was filtered out. Now 10 mL of hexane was added to the filtrate to obtain a reddish yellow precipitate of complex **1a**. Yield: 48 %. Anal. Calcd. For $C_{52}H_{39}ClN_4O_8P_2Ru$ (1046.10): C, 59.69; H, 3.76; N, 5.35. Found: C, 59.39; H, 3.84;

View Article Online
DOI: 10.1039/C6RA17223G

N, 5.28. IR (KBr disk, cm^{-1}): 1880 (ν_{NO}), 1635 (ν_{CONH}), 1092, 620 (ν_{ClO4}), 730, 692, 530 (ν_{PPh3}) cm^{-1}. UV-Vis (CH_2Cl_2; λ_{max}/nm (ε, $M^{-1}cm^{-1}$)): 326 (21370). ^{1}H NMR ($CDCl_3$, 500MHz): δ 9.42 (d, 1H), 9.09 (d, 1H), 8.20 (s, 1H), 7.71 (s, 2H), 7.69–7.53 (m, 17H), 7.45–7.39 (m, 9H), 7.33–7.31 (m, 5H), 7.17–6.95 (m, 2H), 6.52 (s, 1H), 6.13 (d, 1H) ppm. ^{31}P NMR ($CDCl_3$, 500 MHz): δ 29.71 ppm.

Synthesis of [Ru(NO_2L^2)(PPh_3)$_2$(NO)](ClO_4) (2a): Complex **2a** was obtained from complex **2** by following the same procedure as for **1a**. Yield: 51%. Anal. Calcd. For $C_{52}H_{38}Cl_2N_4O_8P_2Ru$ (1080.06): C, 57.79; H, 3.54; N, 5.18. Found: C, 57.56; H, 3.62; N, 5.09. IR (KBr disk, cm^{-1}): 1870 (ν_{NO}), 1585 (ν_{CONH}), 1092, 612 (ν_{ClO4}), 746, 692, 522 (ν_{PPh3}) cm^{-1}. UV-Vis (CH_2Cl_2; λ_{max}/nm (ε, $M^{-1}cm^{-1}$)): 324 (29668). ^{1}H NMR ($CDCl_3$, 500MHz): δ 9.62 (d, 1H), 9.29 (d, 1H), 8.39 (d, 1H), 7.86 (s, 2H), 7.65–7.51 (m, 14H), 7.45–7.34 (m, 11H), 7.24–7.08 (m, 8H), 6.29 (d, 1H) ppm. ^{31}P NMR ($CDCl_3$, 500 MHz): δ 29.73 ppm.

Synthesis of [Ru(NO_2L^3)(PPh_3)$_2$(NO)](ClO_4) (3a): Complex **3a** was prepared from the complex **3** through the same procedure as for **1a**. Yield: 56%. Anal. Calcd. For $C_{52}H_{38}ClN_5O_{10}P_2Ru$ (1091.08): C, 57.23; H, 3.51; N, 6.42. Found: C, 57.14; H, 3.56; N, 6.36. IR (KBr disk, cm^{-1}): 1830 (ν_{NO}), 1645 (ν_{CONH}), 1092, 612 (ν_{ClO4}), 746, 694, 520 (ν_{PPh3}) cm^{-1}. UV-Vis (CH_2Cl_2; λ_{max}/nm (ε, $M^{-1}cm^{-1}$)): 282 (27107), 434 (20867). ^{1}H NMR ($CDCl_3$, 500MHz; J/Hz): δ 10.21 (d, 4.50, 1H), 8.89 (d, 9.00, 1H), 8.50 (d, 9.00, 1H), 8.13 (d, 9.00, 1H), 7.90 (d, 6.50, 5H), 7.65 (d, 8.00, 1H), 7.43–7.31 (m, 15H), and 7.10–7.06 (m, 13H) ppm. ^{31}P NMR ($CDCl_3$, 500 MHz): δ 22.63 ppm.

Synthesis of [Ru(NO_2L^4)(PPh_3)$_2$(NO)](ClO_4) (4a): Complex **4a** was synthesized from complex **4** by using the same procedure as for **1a**. Yield: 62%. Anal. Calcd. For $C_{52}H_{38}ClN_5O_{10}P_2Ru$ (1091.08): C, 57.23; H, 3.51; N, 6.42. Found: C, 57.18; H, 3.60; N, 6.30. IR (KBr disk, cm^{-1}): 1845 (ν_{NO}), 1655 (ν_{CONH}), 1090, 614 (ν_{ClO4}), 742, 692, 514 (ν_{PPh3}) cm^{-1}. UV-Vis (CH_2Cl_2; λ_{max}/nm (ε, $M^{-1}cm^{-1}$)): 288 (30266), 424 (14372). ^{1}H NMR ($CDCl_3$, 500MHz; J/Hz): δ 10.15 (d, 4.50, 1H), 8.89 (d, 9.00, 1H), 8.54 (d, 9.00, 1H), 8.19 (d, 9.00, 1H), 7.97–7.76 (m, 3H), 7.53 (s, 2H), 7.37–7.21 (m, 18H), and 7.11–7.07 (m, 12H) ppm. ^{31}P NMR ($CDCl_3$, 500 MHz): δ 22.35 ppm.

Transfer of NO to myoglobin: 50 mM phosphate buffer solution of 6.8 pH was prepared by adding 0.4192 g of $NaH_2PO_4.2H_2O$ and 0.3283 g of anhydrous Na_2HPO_4 to 50 mL of MilliQ water and making the volume to 100 mL in a volumetric flask. 5 mg equine skeletal muscle myoglobin was dissolved in 5 mL of the above prepared buffer solution.

Griess reagent assay: The photodissociation of nitric oxide from nitrosyl complexes **1a**–**4a** was also confirmed by estimating its amount using the Griess reagent (GR). The reagent was freshly prepared by mixing equal volumes of 1% sulphanilamide in 5% orthophosphoric acid and 0.1% naphthylethylenediamine dihydrochloride (NED) in distilled water. The estimation of NO or nitrite (NO_2^-) ion was measured by observing the increase in the absorbance at ~ 538 nm due to the formation of azo dye.[22,37]

Quantum yield measurements: Standard ferrioxalate actinometer (0.006 M solution of potassium ferrioxalate in 0.1 N H_2SO_4) was used to determine the intensity of the UV light (λ_{irr} = 365 nm). Quantum yields (Φ_{NO}) of NO photorelease for nitrosyl complexes **1a**–**4a** were determined from the decrease in its electronic absorption band with λ_{max} near 326 nm, 324 nm, 434 nmand 424 nm, respectively when irradiated with the light of a UV lamp (λ_{irr} = 365 nm) and were calculated by following the procedure reported earlier.[22] The cuvette was kept 3 cm away from the UV source to measure the quantum yields.

X–ray crystallography: Crystal of complex **4a**.CH_2Cl_2 (reddish yellow) was obtained *via* layering of hexane over a solution of dichloromethane/methanol mixture which is suitable for diffraction study. The X–ray data collection and processing for complex **4a**.CH_2Cl_2 was performed with Bruker Kappa Apex–II CCD diffractometer by using graphite monochromated Mo–Kα radiation (λ = 0.71073 Å) at 296 (2). Crystal structur was solved by direct method. Structure solutions, refinement and data output were carried out with the SHELXTL program.[38,39] All non–hydrogen atoms were refined anisotropically. Hydrogen atoms were placed in geometrically calculated positions and refined using a riding model. Image was created with the DIAMOND program.[40]

Results and Discussion

Syntheses

All the ligands $L^{1-4}H_2$ were obtained in high yield by condensation reaction of different aromatic acids with quinoline-8-amine in dimethylformamide in the presence of 1-hydroxybenzotriazole (HOBT) and dicyclohexylcarbodiimide (DCC).[41] The solid precursor [Ru(PPh_3)$_3Cl_2$] was added to a hot methanol solution (30 mL) of the corresponding ligand $L^{1-4}H_2$ then we obtained the ruthenium(III) complexes [Ru(L^{1-4})(PPh_3)$_2$Cl] (**1**–**4**) (shown in Scheme 3). The complexes **1** and **2** were yellowish brown in color but complexes **3** and **4** werereddish brown and green in color, respectively. Complexes **1**–**4** were highly soluble in dichloromethane, dimethylformamide and dimethylsulphoxide but less soluble in water. The complexes [Ru(NO_2L^{1-4})(PPh_3)$_2$(NO)](ClO_4) (**1a**–**4a**) were derived from the complexes **1**–**4**, respectively (shown in Scheme 3). The dichloromethane solutions of all the complexes **1**–**4** were treated with acidified nitrite ($NaNO_2$) solution with continuous stirring for 2 h and formation of an reddish-yellow color was observed. Then a methanolic solution of $NaClO_4$ was added for the counter anion. All the nitrosyl complexes were found to be reddish yellow in color and were highly soluble in organic solvents like dichloromethane, acetonitrile, dimethylformamide. A dichloromethane/hexane (50:50) mixture was used for recrystallization of nitrosyl complexes **1a**–**4a**. The synthetic procedures described above have been summarized in Scheme 4.

View Article Online
DOI: 10.1039/C6RA17223G

Spectroscopic studies

The infrared (IR) spectra of all the ligands and ruthenium complexes have been recorded by using KBr pellets. In the IR spectrum of ruthenium complexes **1**–**4**, the (–CONH–) stretching frequency (ν_{CONH}) (due to the presence of carbonyl group of carboxamide moiety) was observed near 1558 cm^{-1}, 1635 cm^{-1}, 1632 cm^{-1} and 1625 cm^{-1} for complexes **1**, **2, 3** and **4** respectively,[42–44] which was observed red shifted as compare to the ν_{CONH} values of the free ligands (for L^1H_2, ν_{CONH} = 1674 cm^{-1}; for L^2H_2, ν_{CONH} = 1665 cm^{-1}; for L^3H_2, ν_{CONH} = 1675 cm^{-1}; for L^4H_2, ν_{CONH} = 1670 cm^{-1}) (shown in Figures S1–S8 and Table S1). This red shift indicated the coordination of deprotonated ligands in these cyclometalated complexes and three peaks near 746-742, 694-692 and 520-515 cm^{-1} were examined due to the presence of PPh_3 groups (Table S1).[20–22] On the other hand, the presence of the $\{Ru–NO\}^6$ moiety in all the nitrosyl complexes was confirmed by the characteristic peaks in the infrared spectra. In the IR spectra, the N–O stretching frequencies (ν_{NO}) of nitrosyl complexes **1a**, **2a**, **3a** and **4a** were observed around 1880 cm^{-1}, 1870 cm^{-1}, 1830 cm^{-1} and 1845 cm^{-1} respectively, which were expected for $\{Ru–NO\}^6$ species in the nitrosyl complexes (shown in Figures S9–S16 and Table S1).[20–22,42–44] In the literature, the range of N–O stretching frequencies (ν_{NO}) was reported 1820–1960 cm^{-1} for $\{Ru–NO\}^6$ species.[38] These data were also supported by representative X-ray crystal structure of complex **4a** (vide infra). The values of –CONH– group were found around 1635 cm^{-1}, 1585 cm^{-1}, 1645 cm^{-1} and 1655 cm^{-1} for complexes (**1a**–**4a**), respectively.[42–44] The values of stretching frequencies due to PPh_3 groups (ν_{PPh3}) were observed in the range near 746-730 cm^{-1}, 694-692 cm^{-1} and 530-522 cm^{-1} for the ruthenium nitrosyl complexes **1a**–**4a** (Table S1).[20–22]

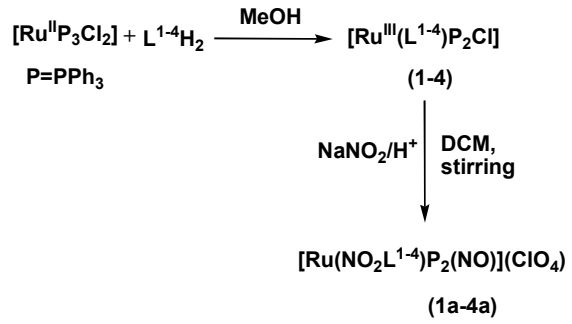

Scheme 4. Synthetic routes for cyclometalaed ruthenium complexes **1–4** and **1a–4a**.

The UV–Vis spectra of ruthenium (III) complexes **1**–**4** were displayed in Figure S17. In complexes **1**–**4**, we observed charge transfer band with λ_{max} near 445 nm as well as 335 nm for complex **1**, 365 nm for complex **2**, 460 nm for **3** and 460 as well as 365 nm for **4** (shown in Figure S17). These bands were probably due to the result of ligand–to–metal charge transfer (LMCT) transition.[32,33,45] In all the complexes **1**–**4,** a charge transfer band was also found around 270 nm which considered as ligand based transition (Table S2).[30,31]

All the nitrosyl complexes **1a**–**4a** were found redish yellow in color and their electronic spectra were displayed in Figure S18. The electronic spectrum of **1a–4a** gave rise to charge-transfer band near 326 nm, 324 nm, 434 nm, and 424 nm, respectively which was recognized to a metal to ligand charge transfer (MLCT) transition $d\pi(Ru)\rightarrow\pi^*(NO)$ type and this transition has been responsible for the photolability of the $\{RuNO\}^6$ moiety.[6,7,46] In the complexes **3a** and **4a**, we also found a charge transfer band near 282 nm and 288 nm, respectively (Table S2).

All the ruthenium nitrosyl complexes **1a**–**4a** were found to be diamagnetic which were confirmed by ^1H and ^{31}P NMR spectral studies. The ^1H and ^{31}P NMR spectra of nitrosyl complexes **3a** and **4a** were displayed in Figures S19–S26. In all the ligands, we observed a peak near 10.75 ppm which was due to the presence of carboxamido (–CONH–) proton. But in the nitrosyl complexes, no peak was obtained around 10.75 ppm which indicated the absence of –NH– proton of carboxamido (–CONH–) group in these nitrosyl complexes and we obtained other expected multiple signals near 10.20–7.00 ppm range (Table S3).[41] We obtained a single peak near 30.0 ppm (for **1a**, **2a**) and 22.0 ppm (for **3a**, **4a**) in ^{31}P NMR spectra which indicated the presence of *trans* PPh_3 groups in all the nitrosyl complexes **1a**–**4a** (Table S3).[20–22] These ^{31}P NMR data were also consistent with X-ray crystal structure (*vide infra*).

We would like to mention here that we were unable to generate a good ^1H NMR spectra for **1a** and **2a** although the same for complexes **3a** and **4a** were reasonable. ^{31}P NMR data are ~22ppm for **1a** and **2a** whereas ~30ppm for **3a** and **4a**. This prompted us to have a closer look to ν_{NO} and ^{31}P NMR data along with ^1H NMR spectra (Table S4 in supporting information). These data clearly express that complexes **1a** and **2a** are having one type of electronic structure and complexes **3a** and **4a** possess a different type of electronic structure. All the complexes contain $\{Ru–NO\}^6$ moiety[6] and $\{Ru^{II}–NO^+\}^6$ description was suggested.[6] However $\{Ru^{II}–NO^+\}^6$ description predicts complete transfer of electron density from NO to ruthenium. This may vary for different complexes depending upon the other ligands present in the complex. Presence of $–NO_2$ group in the ligand frame probably facilitates complete transfer and formation of diamagnetic $\{Ru^{II}–NO^+\}^6$ (for complexes **3a** and **4a**). The substituents are different (-H and -Cl) for complexes **1a** and **2a** and hence they have different electronic structure. These are the probable reasons for the bad ^1H NMR signals and shift in ^{31}P NMR spectra for **1a** and **2a**.

Description of molecular structure

The molecular structure of the complex $[Ru(NO_2L^4)(PPh_3)_2(NO)](ClO_4).CH_2Cl_2$ (**4a**. CH_2Cl_2) is depicted in Figure 1. The selected bond lengths and bond angles of complex **4a**.CH_2Cl_2 are given in Table 1. Crystal data collection and refinement detail of the structure of complex **4a**.CH_2Cl_2 is summarized in Table 2.

In the crystal structure of **4a**·CH_2Cl_2, the equatorial plane was involved of carbanion (C2), Cl(1), pyridine nitrogen (N2)

View Article Online
DOI: 10.1039/C6RA17223G

and NO. We observed that both the phosphine groups were *trans* to each other which was supported by ^{31}P NMR spectral data. The ruthenium center adopted a distorted-octahedral

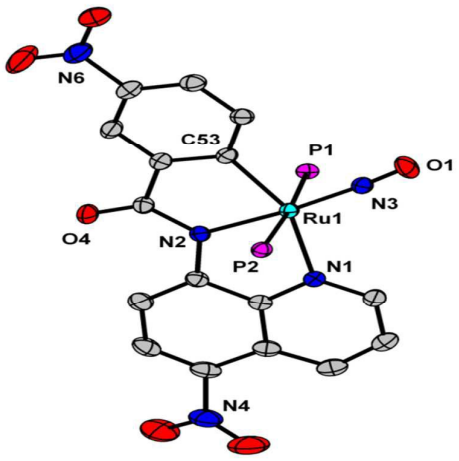

Figure 1. ORTEP diagram (30% probability level) of the cation of the $[Ru(NO_2L^4)(PPh_3)_2(NO)](ClO_4).CH_2Cl_2$ (**4a**.CH_2Cl_2). All hydrogen atoms, solvent molecule and all the phenyl rings of PPh_3 groups are omitted for clarity.

geometry. The nitrogen atom of carboxamido (–CONH) ligand was coordinated to the metal center and the ruthenium-carboxamido nitrogen (Ru(1)–N(2)) bond distance (2.042(2) Å) was found to be closer to the reported values.[42,44,47] The Ru–C(53) (2.068(3) Å) distance was also consistent with the values reported in the literature[22,30] and found to be very close to the bond length reported by Pal and coworkers.[31] In this structure, the carboxamido nitrogen atom (–CONH–) was bound to the metal center so there was no peak of amide hydrogen atom in the ^{1}H NMR spectrum.

Table 1. Selected bond lengths (Å) and bond angles (deg.) of complex **4a**·CH_2Cl_2.

Bond lengths (Å)		Bond angles (°)	
Ru(1)–C(53)	2.068(3)	N(2)–Ru(1)–N(3)	174.69(9)
Ru(1)–N(1)	2.176(2)	N(2)–Ru(1)–C(53)	79.63(10)
Ru(1)–N(2)	2.040(2)	N(1)–Ru(1)–N(2)	76.66(8)
Ru(1)–P(1)	2.4710(7)	N(3)–Ru(1)–P(1)	92.51(7)
Ru(1)–P(2)	2.4647(7)	N(3)–Ru(1)–P(2)	91.53(7)
Ru(1)–N(3)	1.759(2)	P(1)–Ru(1)–P(2)	175.52(2)
N(3)–O(1)	1.139(3)	O(1)–N(3)–Ru(1)	175.3(2)

Quinoline shows the chemistry of benzene as well as pyridine and electrophilic substitution occurs at the benzene ring whereas nucleophilic substitution takes place at the pyridine ring.[48] It is well known in the literature[49] that nuclear nitration for simple aromatic compounds proceeds *via* electrophilic pathway. So ligand nitration ($–NO_2$) was found on the phenyl ring of quinoline containing the amine function and the site of nitration was *trans* to the amine group.

In the nitrosyl complex, $Ru–N_{NO}$ (1.759(2) Å)[20–22] and N–O (1.139(2) Å)[20,22] bond distances were obtained similar to the reported values in the literature. The N–O stretching frequency and N–O distance along with Ru–N–O angle (~175°) clearly expressed $\{Ru^{II}–NO^{+}\}^6$ description of $\{Ru–NO\}^6$ moiety in the nitrosyl complex.[20–22] These data were supported through IR spectroscopic studies and the presence of *trans*-phosphine groups were also indicated by ^{31}P NMR data. Ru–N(1) (pyridine nitrogen) and Ru–P distances were also close to the values already reported.[20,22]

Table 2. Summary of crystal data and structural refinement parameters for complex **4a**·CH_2Cl_2.

Empirical formula	$C_{53}H_{40}Cl_3N_5O_{10}P_2Ru$
Formula weight	1176.26
Temperature /K	296(2)
λ (Å) (Mo-Kα)	0.71073
Crystal system	Triclinic
Space group	*P* –1
A (Å)	12.0096(5)
B (Å)	12.6429(5)
C (Å)	19.2406(8)
α (°)	81.340(2)
γ (°)	64.743(2)
β (°)	86.300(2)
V (Å^3)	2612.02(19)
Z	2
ρ_{calc} (gcm^{-3})	1.496
F(000)	1196
Theta range	1.07–28.34
Index ranges	−11< *h*< 16, −16< *k*< 16, −25< *l*< 25
Data/restraints/par.	13031/0/668
GOF[a] on F^2	1.211
*R*1[b] [$I > 2\sigma(I)$]	0.0456
*R*1[all data]	0.0567
*wR*2[c] [$I > 2\sigma(I)$]	0.1458
*wR*2 [all data]	0.1631

[a]GOF = $[\Sigma[w(F_o^2 – F_c^2)^2] /M – N]^{1/2}$ (M = number of reflections, N = number of parameters refined). [b]$R1 = \Sigma \| |F_o| – |F_c| \| / \Sigma |F_o|$. [c]$wR2 = [\Sigma[w(F_o^2 – F_c^2)^2] / \Sigma [(F_o^2)^2]]^{1/2}$.

Site Specific Orthometallation: A Reaction Model

The reaction of $Ru(PPh_3)_3Cl_2$ with ligands having amide bond afforded cyclometalated ruthenium complexes *via* C–H bond activation and orthometallation. During this reaction, we observed that the orthometallation happened in the phenyl ring of benzoic acids. However it is important to note here that in case of m-nitrobenzoic acid, there are two probable sites accessible for C–H bond activation and orthometallation. This is a situation similar to our previous results.[22] After the completion of reaction, we observed only a single orthometallated product. In resultant ruthenium organometallics, the nitro group was found to be at a para

View Article Online
DOI: 10.1039/C6RA17223G

position with respect to orthometallated carbon. According to the literature, at the time of orthometallation, the metal centre could act as a nucleophile or an electrophile.[22,50–52]

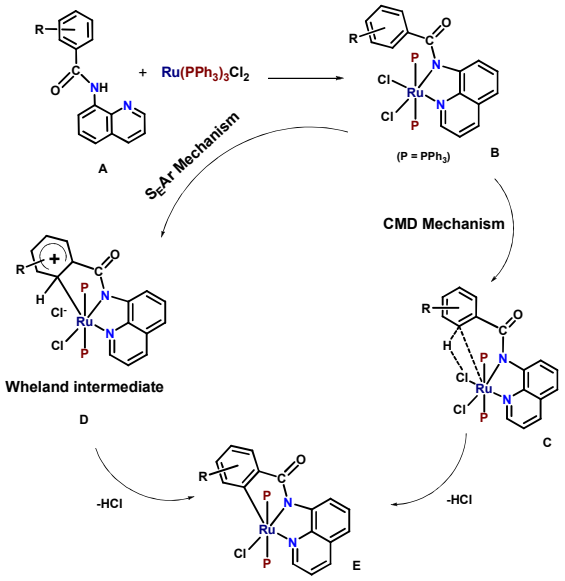

Scheme 5. Proposed reaction model for cyclometalation.

In the present study the precursor ruthenium complex contains Ru(II) centre and coordination of deprotonated amide nitrogen will stabilize Ru(III). In higher oxidation state metal centre behaves as an electrophile and Ru-C bond is formed via C–H bond activation.

Investigation of literature [50,57] revealed that different reaction pathways were proposed for C⁻H bond activation and metal-carbon bond formation. Electrophilic aromatic substitution (S_EAr) and concerted metalation-deprotonation (CMD) are the two important reaction pathways that have received most attention in this regard.[57] In the S_EAr mechanism, reaction proceeds via formation of Wheland intermediate. In Wheland intermediate a metal ion is bound to the carbon atom of the arene via a covalent bond and metal–carbon bond is formed before the C⁻H bond is cleaved. In a CMD transition state, metal bound chloride ion abstracts a proton from C⁻H bond while, at the same time, a metal carbon bond is being formed. Hence we propose a possible reaction model in Scheme 5.

Electrochemistry

We have investigated the redox properties of ruthenium center in complexes **1–4** and **1a–4a** with the help of cyclic voltammetric studies. In the voltammograms of precursor the complexes (**1–4**), we found quasi-reversible redox couples with $E_{1/2}$ values near +0.56 V (for **1**), +0.60 V (for **2**), +0.92 V (for **3**) and +0.92 V (for **4**) *vs*. Ag/AgCl which were attributed to Ru(III)/Ru(IV) couples (Figure 2).[22,30,31] In case of complexes **3** and **4**, we also obtained quasi-reversible redox couples near–0.37V and –0.32 V *vs*. Ag/AgCl respectively which were assigned as Ru(III)/Ru(II) couple (Figure 2).[22,31,32] The results obtained for precursor complexes (**1**–**4)** clearly indicated better stability of Ru(III) center in case of complexes **3** and **4**. This happened probably due to the presence electron withdrawing group ($–NO_2$) in the ligand frame. In case of complex **4**, slightly less $E_{1/2}$ value of Ru(III)/Ru(II) response was found as compare to the $E_{1/2}$ value of complex **3** indicated that the presence of $–NO_2$ with respect to carbanion (*para* or *meta*) could not be ignored (Figure 2). In case of ruthenium nitrosyl complexes **1a** and **2a**, we did not observed any redox couple but found only cathodic peak near –1.09 V and –0.96 V, respectively (Figure 3). Lahiri and coworkers explained ligand (nitric oxide) centered reduction of $(Ru^{II}–NO^{+})^6/(Ru^{II}–NO^{\cdot})^7$ and then second reduction for the appearance of such type two peaks at negative potentials.[53] In the cyclic voltammogram of complex **3a**, we obtained two redox couple near –0.68 V and –1.00 V *vs*. Ag/AgCl. In case of complex **4a**, two redox couples were also exhibited near –0.67 V and –1.02 V *vs*. Ag/AgCl. (Figure 3). In the negative potential quasi-reversible couples(Ru^{III}/Ru^{II}) for nitrosyl complexes were reported by Mascharak and coworkers.[44,54]

Photolysis experiments for ruthenium nitrosyl complexes

ll the nitrosyl complexes **1a**–**4a** were found to be photolabile under light and the photolability of coordinated NO of nitrosyl complexes was performed under visible as well as UV light.

View Article Online
DOI: 10.1039/C6RA17223G

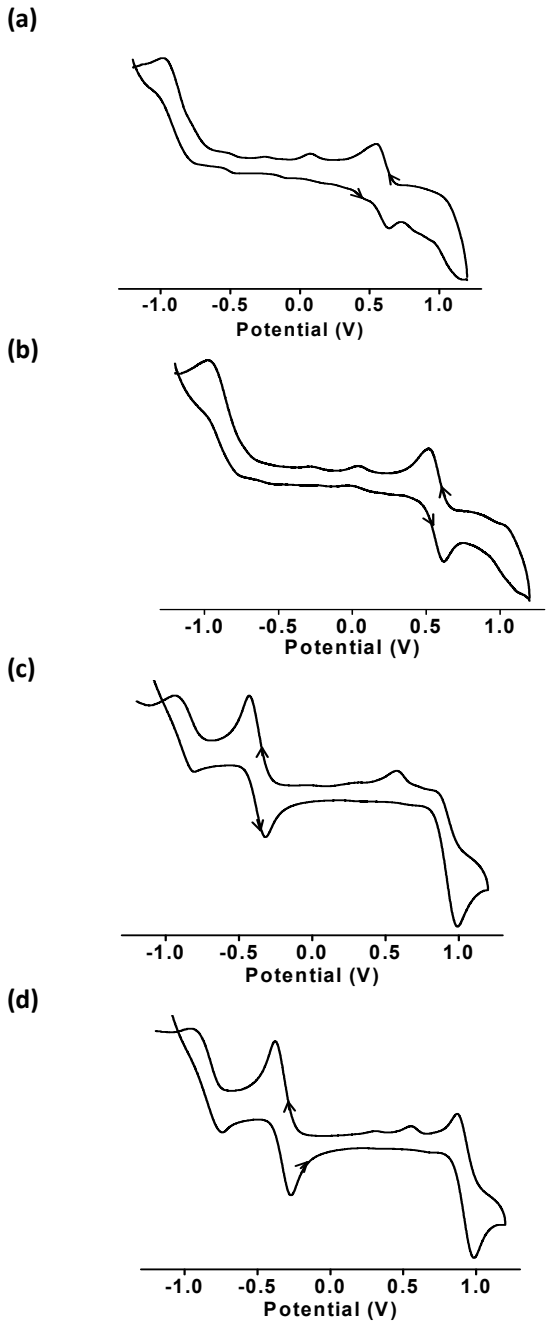

Figure 2. Cyclic voltammograms of 10^{-3} M solutions of (a) complex **1**, (b) complex **2**, (c) complex **3**, (d) complex **4** in dichloromethane in presence of 0.1 M tetrabutylammonium perchlorate (TBAP) using working electrode, glassy-carbon; reference electrode, Ag/AgCl; auxiliary electrode, platinum wire and scan rate, 0.1 V/s.

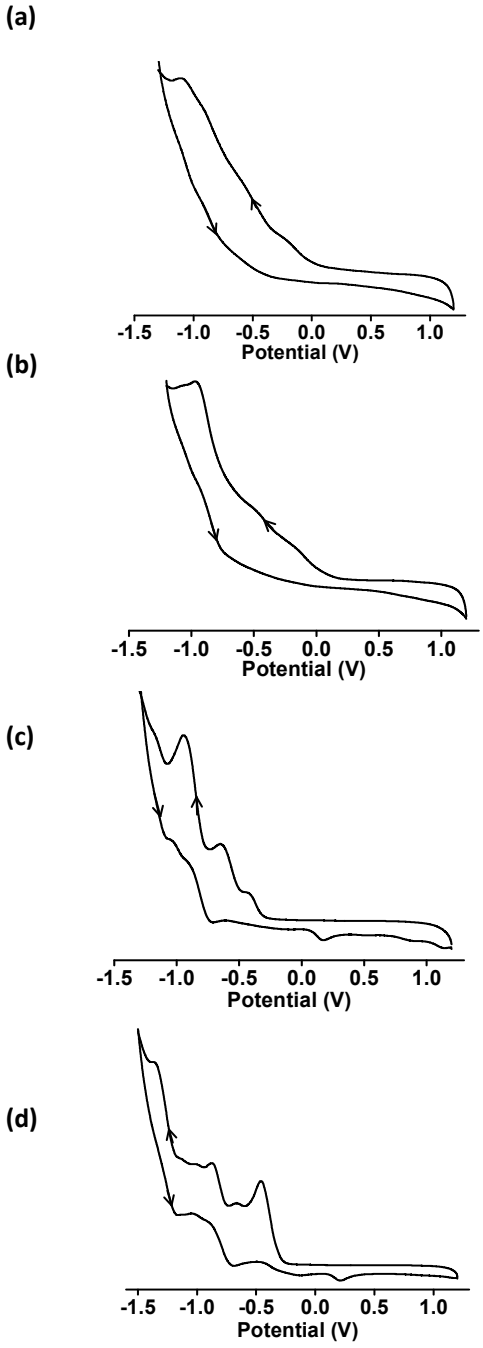

Figure 3. Cyclic voltammograms of 10^{-3} M solutions of (a) complex **1a**, (b) complex **2a**, (c) complex **3a**, (d) complex **4a** in dichloromethane in presence of 0.1 M tetrabutylammonium perchlorate (TBAP) using working electrode, glassy-carbon; reference electrode, Ag/AgCl; auxiliary electrode, platinum wire and scan rate, 0.1 V/s

View Article Online
DOI: 10.1039/C6RA17223G

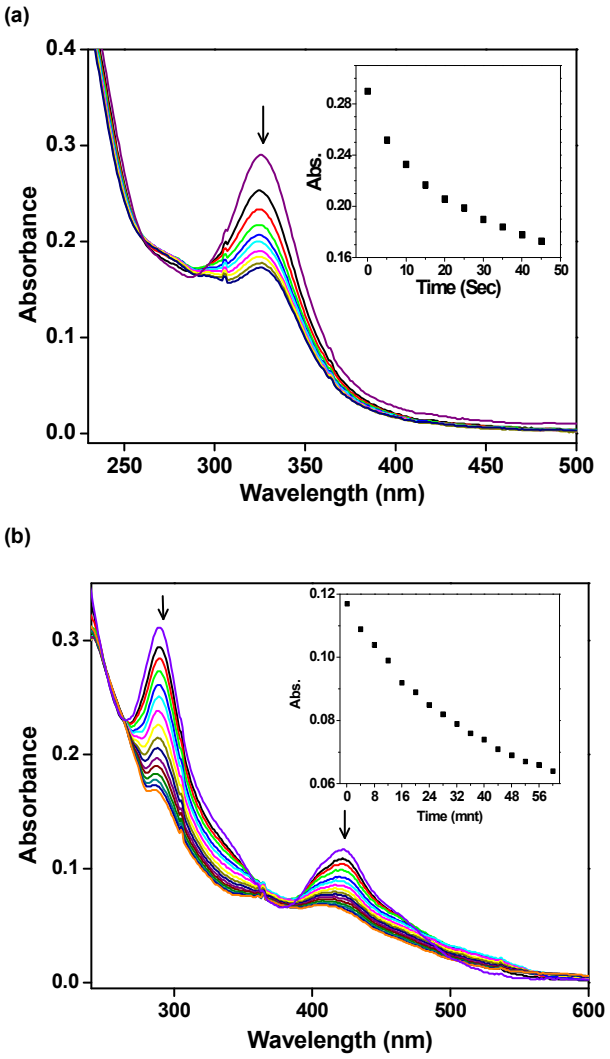

Figure 4. Photodissociation of NO from complexes (a) **1a** (~ 1.5 x 10^{-5} M) and (b) **4a** (~ 1.2 x 10^{-5} M) in dichloromethane solutions under illumination with a UV light (λ_{irr} = 365 nm). Repetitive scans were taken in 5 seconds intervals for **1a** and in 4 minutes intervals for **4a**.Inset: Changes in absorbance with time at λ = 326 nm and λ = 424 nm for **1a** and **4a** respectively at room temperature.

In dark condition, there was no color change observed. On the other hand in the presence of light we observed a color change from reddish-yellow to reddish brown. In the presence of visible light (100 Watt tungsten lamp), we did not observed much change in the UV-Vis spectra of nitrosyl complexes. However, rapid spectral changes were observed when the solutions were exposed to low intensity light of the UV lamp (λ_{irr} = 365 nm). A dichloromethane solution of complex **1a** was exposed to low intensity UV light and we observed the disappearance of a peak near 326 nm. These results are indicative of photolability of coordinated NO (Figure 4(a)).In case of complex **2a**, we also observed the same disappearance of a peak near 324 nm (shown in Figure S 27). When a solution of complex **3a** was illuminated under UV light, we obtained a decrease in peak intensities near 435 as well as 282 nm and we found two isobestic points near 482 nm and 350 nm (shown in Figure S 28). The spectral changes were also observed with complex **4a** in the dichloromethane solution. In this case, we also found a decrement in peak intensities near 424 nm as well as 288 nm under UV light (Figure 4(b)).

Trapping of photoreleased NO by reduced myoglobin

The photocleavage of coordinated NO from ruthenium nitrosyl complexes was also confirmed by trapping the liberated NO by

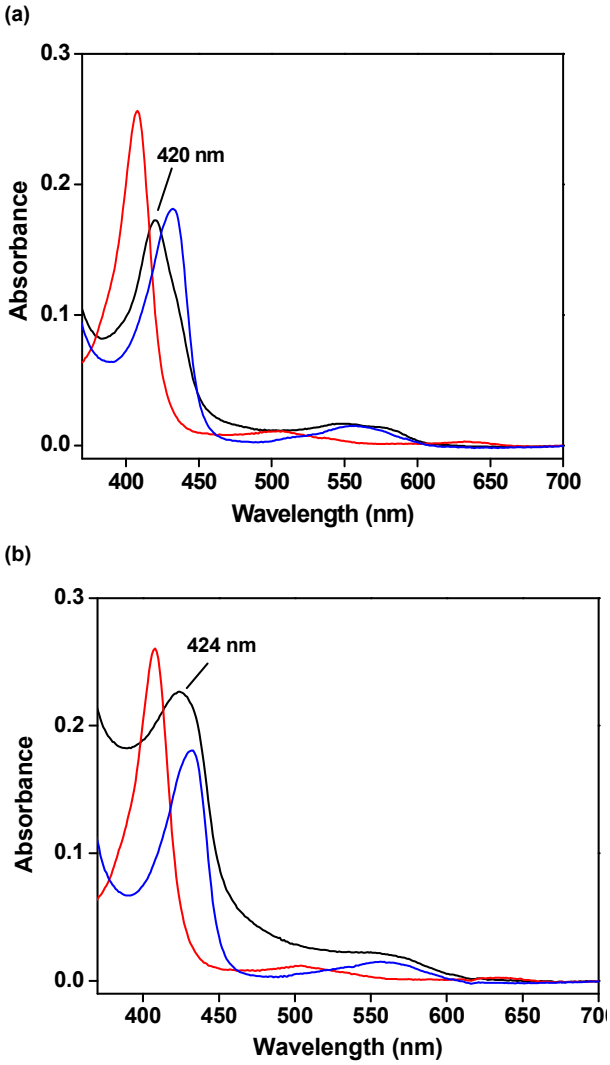

Figure 5. Electronic spectra for conversion of reduced Mb to Mb–NO adducts upon reaction with **3a** and **4a** in buffer solutions (50 mM phosphate buffer, pH 6.8) under exposure of

View Article Online
DOI: 10.1039/C6RA17223G

UV light (λ_{irr} = 365 nm). Red line, oxidized Mb (intense band at ~ 409 nm); blue line, reduced Mb (at ~ 433 nm, with excess of sodium dithionite). **(a)** Black line, Mb–NO adduct (at ~ 420 nm), obtained by Mb and solution of **3a** (~ 10^{-5} M) exposed to UV light for 2-3 minutes. **(b)** Black line, Mb–NO adduct (at ~ 424 nm) obtained by Mb and solution of complex **4a** (~4.3 x 10^{-5} M) exposed to UV light for 10-11 minutes.

reduced myoglobin (Mb) using low intensity UV lamp in phosphate buffer (pH ~ 6.8).[22] In electronic absorption spectra, we obtained an intense band at 409 nm (Soret band) for oxidized myoglobin (Mb). In the same solution, the sodium dithionite was added in excess and then we obtained an intense band near ~ 433 nm in the UV-Vis spectra due to the reduced myoglobin. Acetonitrile solution of nitrosyl complexes were added to a solution containing reduced myoglobin and no reaction was obtained under dark conditions. However, when the same solution was illuminated with UV light (λ_{irr} = 365 nm) for 2-3 minutes then absorption spectra at near 420 nm (for **1a** near 421, for **2a** near 424 (Figure S29) and for **3a** 420 (Figure 5(a))) clearly indicated the formation of Mb–NO adducts.[20–22] However in case of **4a**, the same solution mixture was kept under exposure to the light of UV lamp for 10-11 minutes then we observed a band near 424 nm in UV-Vis spectra indicating the formation of Mb–NO adduct (Figure 5(b))[20–22] with a longer exposure to light.

Estimation of photoreleased NO by Griess reaction

We estimated the amount of photoliberated NO from ruthenium nitrosyl complexes in the presence of UV light (λ_{irr} = 365 nm) by using Griess reagent assay.[22,34,37] The photolability of NO in complexes **1a–4a** was further observed through increasing in optical density of the produced azo dye at ~ 538 nm in the presence of ultraviolet light. In dark conditions, a little amount of NO was found to be released. When the solutions of complexes **1a–4a** (50 μM) with Griess reagent was exposed with UV light for 15 minutes then the amount of NO was liberated ~ 5.2 μM (for **1a**), ~ 4.6 μM (for **2a**, Figure S30), ~ 6.3 μM (for **3a**, Figure 6(a)) and ~ 5.0 μM (for **4a**, Figure 6(b)). The change in absorbance spectra of produced azo dye was found to be small under visible light (100 Watt tungsten lamp) (Figure S31 and Table 3). The results of estimated NO from our nitrosyl complexes were compared with the data obtained from sodium nitroprusside (SNP), a standard nitric oxide (NO) donor[6,55,56] in same experimental conditions. In ultraviolet light (low intensity), 50 μM solution of sodium nitroprusside released ~ 3.4 μM of nitric oxide (Table 3). These data gave rise to the formation of NO and the amount of photoreleased NO form complexes **1a**–**4a** was found to be close to the amount of NO released by SNP under UV light. Interestingly **4a** gave rise to roughly similar amount of NO under visible as well as UV light (Figure S32). This is probably due to extended delocalization of charge from NO →Ru→phenyl ring→NO_2 (para with respect to carbanion).

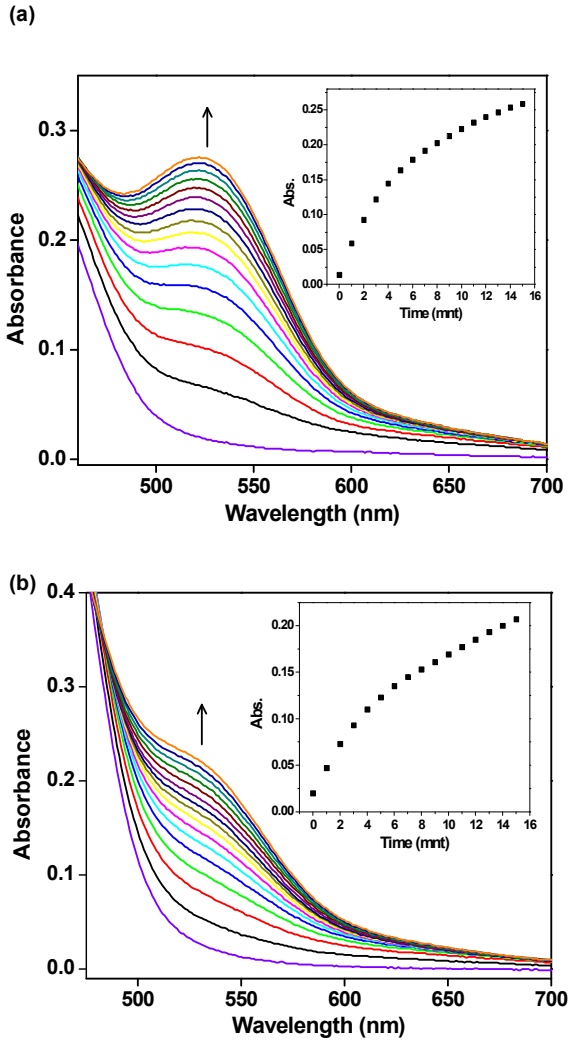

Figure 6. Electronic spectra of dye formation when Griess reagent (100 μL) was treated with complexes (a) **3a** (50 μM) (b) **4a** (50 μM) in the presence of UV light (λ_{irr} = 365 nm). Repetitive scans were taken in 1 minute intervals. Inset: Time dependent changes in absorbance at λ_{irr} = 538 nm at room temperature.

Table 3 Estimation of NO production from **1a**, **2a**, **3a**, **4a** and sodium nitroprusside (SNP) in Griess reagent assay.

Complex	Complex conc.	NO produced (μM)[a] Griess reaction		
		Dark	Visible light	UV light
1a	50 μM	0.42	2.4	5.2
2a	50 μM	0.50	3.6	4.6
3a	50 μM	0.30	3.1	6.3
4a	50 μM	0.48	5.8	5.0
SNP	50 μM	0.04	0.2	3.4

[a] Average of three experiments.

View Article Online
DOI: 10.1039/C6RA17223G

Conclusions

The following are the major findings of the present study. First, a different combination of donor atoms (pyridyl nitrogen and amide nitrogen) were utilized to investigate the C–H bond activation and the bidentate ligand was converted to a tridentate one with the formation of Ru–C bond. These data and our previous results clearly indicate that the presence of at least one Ru(III) stabilizing donor in the ligand frame was necessary to afford orthometallation and synthesis of Ru(III) organometallic complexes. Second, new family of ruthenium(III) cyclometalate complexes $[Ru(L^{1-4})(PPh_3)_2Cl]$ (**1–4**) were obtained *via* C–H bond activation and were characterized by different spectroscopic studies. The ligand frame utilized in this report is related to the works by Chatani and coworkers.[4] and in the propose mechanism they have mentioned the formation of Ru–C bond via C–H activation (intermediate 32, in Scheme 1 in reference 4) during C–C bond formation. To the best of our knowledge there is no structural characterization of intermediate 32. Hence this is the first example of structurally characterized intermediate which clearly show the site specific C–H activation. Third, nitric oxide (NO) reactivity studies previously gave rise to the coordination of NO in *trans* position to carbanion. Here, two groups present in the ligand are carboxamido (–CONH–) and carbanion groups, which exhibit *trans* effect. We found the dissociation of chloride ion from the metal centre which was situated in *trans* position to deprotonated nitrogen of carboxamido group and then NO was coordinated to the metal centre to afford ruthenium nitrosyl complexes $[Ru(NO_2L^{1-4})(PPh_3)_2(NO)](ClO_4)$ (**1a–4a**) and these nitrosyl complexes were characterized by spectroscopic studies. The molecular structure of representative complex **4a** was examined by X–ray crystallography. Fourth, ligand nitration was also observed in the activated phenyl group containing $–NH_2$ function in the qunoline moiety. Fifth, resultant nitrosyl complexes were found to be photosensitive under visible as well as UV light and we have also investigated the liberation of NO by trapping experiment with the help of reduced myoglobin. We have quantified the amount of photoreleased nitric oxide (NO) by using Griess reaction. Sixth, we have observed that in the complexes **1a**, **2a** and **3a** released nitric oxide easily under visible as well as UV light and the amount of NO released under UV light was more as compare to NO released under visible light. Complex **4a** provided roughly same amount of NO under UV and visible light. We are trying to modify the ligand to observe photorelease of NO in the desired range 700-1000 nm and work is under progress.

Acknowledgements

KG is thankful to CSIR, New Delhi, India for financial assistance no. (01(2720)/13/EMR–II dated 17–04–2013). RK, SK and MB are thankful to CSIR, New Delhi and AR is thankful to MHRD for their fellowships. U. P. S. is thankful for support by single-crystal X-ray facility of the IIT Roorkee.

Notes and references

1 P. B. Arockiam, C. Bruneau, P. H. Dixneuf, *Chem. Rev.* 2012, **112**, 5879.
2 V. Ritleng, C. Sirlin, M. Pfeffer, *Chem. Rev.* 2002, **102**, 1731.
3 P. G. Bomben, K. C. D. Robson, B. D. Koivisto, C. P. Berlinguette, *Coord. Chem. Rev.* 2012, **256**, 1438.
4 Y. Aihara, N. Chatani, *Chem. Sci.* 2013, **4**, 664.
5 Y. Zhao, C. Snieckus, *Adv. Synth. Catal.* 2014, **356**, 1527.
6 M. J. Rose, P. K. Mascharak, *Coord. Chem. Rev.* 2008, **252**, 2093 and references therein.
7 N. L. Fry, P. K. Mascharak, *Acc. Chem. Res.* 2011, **44**, 289 and references therein.
8 U. Schatzschneider, *Eur. J. Inorg. Chem.* 2010, 1451.
9 P. C. Ford, *Nitric Oxide* 2013, **34**, 56.
10 N. L. Fry, P. K. Mascharak, *Dalton Trans.* 2012, **41**, 4726.
11 S. Sarkar, B. Sarkar, N. Chanda, S. Kar, S. M. Mobin, J. Fiedler, W. Kaim, G. K. Lahiri, *Inorg. Chem.* 2005, **44**, 6092.
12 P. De, B. Sarkar, S. Maji, A. K. Das, E. Bulak, S. M. Mobin, W. Kaim, G. K. Lahiri, *Eur. J. Inorg. Chem.* 2009, 2702.
13 A. D. Chowdhury, P. De, S. M. Mobin, G. K. Lahiri, *RSC Adv.* 2012, **2**, 3437.
14 M. G. Sauaia, R. G. de Lima, A. C. Tedesco, R. S. da Silva, *J. Am. Chem. Soc.* 2003, **125**, 14718.
15 M. G. Sauaia, R. G. de Lima, A. C. Tedesco, R. S. da Silva, *Inorg. Chem.* 2005, **44**, 9946.
16 F. Roncaroli, M. Videla, L. D. Slep, J. A. Olabe, *Coord. Chem. Rev.* 2007, **251**, 1903.
17 M. Sieger, B. Sarkar, S. Zalis, J. Fiedler, N. Escola, F. Doctorovich, J. A. Olabe, W. Kaim, *Dalton Trans.* 2004, 1797.
18 F. A. Cotton, G. Wilkinson, "Advanced inorganic chemistry" 5th ed.; Wiley, New York, 1930.
19 H. Hadadzadeh, M. C. DeRosa, G. P. A. Yap, A. R. Rezvani, R. J. Crutchley, *Inorg. Chem.* 2002, **41**, 6521.
20 K. Ghosh, S. Kumar, R. Kumar, U. P. Singh, N. Goel, *Inorg. Chem.* 2010, **49**, 7235.
21 K. Ghosh, S. Kumar, R. Kumar, U. P. Singh, N. Goel, *Organometallics* 2011, **30**, 2498.
22 K. Ghosh, S. Kumar, R. Kumar, U. P. Singh, *Eur. J. Inorg. Chem.* 2012, 929.
23 K. Ghosh, R. Kumar, S. Kumar, M. Bala, U. P. Singh, *Transition Met. Chem.* 2015, *40*, 831.
24 G. K. Lahiri, S. Bhattacharya, M. Mukherjee, A. K. Mukherjee, A. Chakravorty, *Inorg. Chem.* 1987, **26**, 3359.
25 G. Venkatachalam, R. Ramesh, *Tetrahedron Lett.* 2005, **46**, 5215.
26 G. Venkatachalam, R. Ramesh, S. M. Mobin, *J. Organomet. Chem.* 2005, **690**, 3937.
27 S. Kannan, R. Ramesh, Y. Liu, *J. Organomet. Chem.* 2007, **692**, 3380.
28 P. Ghosh, A. Pramanik, N. Bag, G. K. Lahiri, A. Chakravorty, *J. Organomet. Chem.* 1993, **454**, 237.
29 P. Munshi, R. Samanta, G. K. Lahiri, *J. Organomet. Chem.* 1999, **586**, 176.
30 R. Raveendran, S. Pal, *J. Organomet. Chem.* 2007, **692**, 824.
31 R. Raveendran, S. Pal, S. *J. Organomet. Chem.* 2009, **694**, 1482.
32 K. Nagaraju, S. Pal, *J. Organomet. Chem.* 2013, **737**, 7.
33 K. Nagaraju, S. Pal, *J. Organomet. Chem.* 2013, **745–746**, 404.
34 K. Ghosh, R. Kumar, S. Kumar, J. S. Meena, *Dalton Trans.* 2013, **42**, 13444.
35 K. Ghosh, A. A. Eroy-Reveles, B. Avila, T. R. Holman, M. M. Olmstead, P. K. Mascharak, *Inorg. Chem.* 2004, **43**, 2988.
36 T. A. Stephenson, G. J. Wilkinson, *J. Inorg. Nucl. Chem.* 1966, **28**, 945.
37 K. Ghosh, R. Kumar, K. Kumar, A. Ratnam, U. P. Singh, *RSC Adv.* 2014, **4**, 43599.

View Article Online
DOI: 10.1039/C6RA17223G

38 G. M. Sheldrick, *Acta Crystallogr., Sect. A: Found. Crystallogr.*, 1990, **46**, 467.
39 G. M. Sheldrick, *SHELXTL-NT 2000 version 6.12*, Reference Manual, University of Gottingen, Pergamon, New York, 1980.
40 B. Klaus, *DIAMOND, Version 1.2 c*, University of Bonn, Germany, **1999**.
41 K. Ghosh, S. Kumar, R. Kumar, U. P. Singh, *J. Organomet. Chem*. 2014, **750**, 169.
42 A. K. Patra, M. J. Rose, K. A. Murphy, M. M. Olmstead, P. K. Mascharak, *Inorg. Chem*. 2004, **43**, 4487.
43 N. L. Fry, B. J. Heilman, P. K. Mascharak, *Inorg. Chem*. 2011, **50**, 317.
44 M. J. Rose, A. K. Patra, E. A. Alcid, M. M. Olmstead, P. K. Mascharak, *Inorg. Chem*. 2007, **46**, 2328.
45 K. Ghosh, S. Kumar, R. Kumar, *Eur. J. Inorg. Chem*. 2014, 1454.
46 K. Ghosh, S. Kumar, R. Kumar, *Inorg. Chim. Acta* 2013, **405**, 24.
47 N. L. Fry, M. J. Rose, D. L. Rogow, C. Nyitray, M. Kaur, P. K. Mascharak, *Inorg. Chem*. 2010, **49**, 1487.
48 J. Clayden, N. Greeves, S. Warren, P. Wothers, *Organic Chemistry*, Oxford University Press, 2001.
49 S. Chattopadhyay, K. Ghosh, S. Pattanayak, A. Chakravorty, *Dalton Trans* 2001, 1259 and references therein.
50 N. Chitrapriya, V. Mahalingam, M. Zeller, K. Natarajan, *Polyhedron* 2008, **27**, 1573.
51 R. L. Brainard, W. R. Nutt, T. R. Lee, G. M. Whitesides, *Organometallics* 1988, **7**, 2379.
52 R. Cordone, W. D. Harman, H. Taube, *J. Am. Chem. Soc*. 1989, **111**, 2896.
53 S. Maji, B. Sarkar, M. Patra, A. K. Das, S. M. Mobin, W. Kaim, G. K. Lahiri, *Inorg. Chem*. 2008, **47**, 3218.
54 A. K. Patra, P. K. Mascharak, *Inorg. Chem*. 2003, **42**, 7363.
55 A. A. Eroy-Reveles, Y. Leung, C. M. Beavers, M. M. Olmstead, P. K. Mascharak, *J. Am. Chem. Soc*. 2008, **130**, 4447.
56 C. Xin Zhang, S. J. Lippard, *Curr. Opin. Chem. Biol*. 2003, **7**, 481.
57 S. I. Gorelsky, *Coord. Chem. Rev*. 2013, **257**, 153.

View Article Online
DOI: 10.1039/C6RA17223G

Graphical Abstract Pictogram

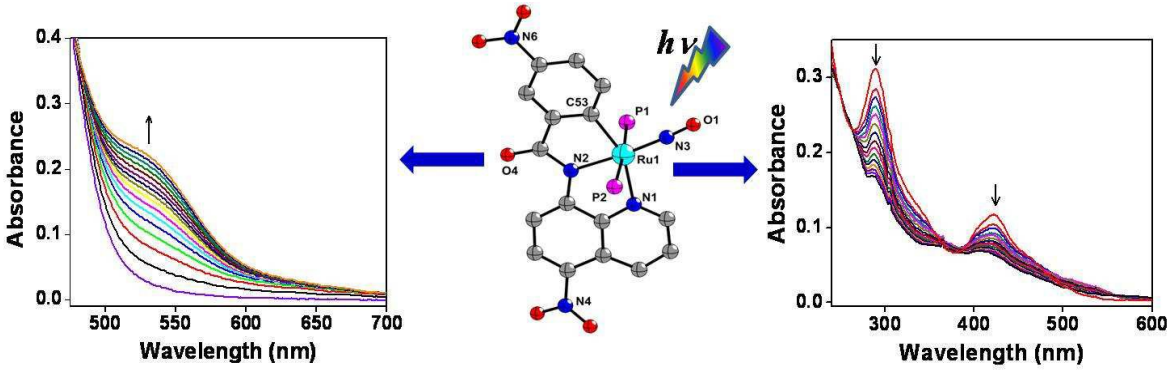

Graphical Abstract Synopsis

A new family of σ-aryl ruthenium(III) complexes derived from the bidentate ligands having amide bond through C–H bond activation were synthesized. These organometallic complexes were treated with nitric oxide (NO) to afford organometallic nitrosyl complexes. All the ruthenium complexes were characterized by various spectroscopic techniques and electrochemical studies. The molecular structure of representative complex was established by X-ray crystallography. Nitric oxide molecule was found to be photolabile in these nitrosyl complexes under light.